

Self-organized nanoscale Ge dots and dashes on SiGe/Si superlattices

Cite as: J. Appl. Phys. **98**, 024317 (2005); <https://doi.org/10.1063/1.1993751>

Submitted: 04 January 2005 • Accepted: 09 June 2005 • Published Online: 01 August 2005

L. Fitting, M. E. Ware, J. R. Haywood, et al.



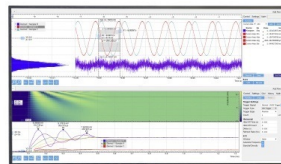
View Online



Export Citation

Challenge us.

What are your needs for
periodic signal detection?



Zurich
Instruments

Self-organized nanoscale Ge dots and dashes on SiGe/Si superlattices

L. Fitting, M. E. Ware, J. R. Haywood, Jennifer J. H. Walter, and R. J. Nemanich^{a)}

Department of Physics, North Carolina State University, Raleigh, North Carolina 27695-8202

(Received 4 January 2005; accepted 9 June 2005; published online 1 August 2005)

This study explores the self-organization of Ge nanostructures on SiGe/Si superlattices grown on Si substrates with the surface normal tilted from (001) towards (111) by up to 25°. Prior studies found two-dimensional ordering of Ge dots on nominally flat Si(001) surfaces with a very homogeneous size distribution. Our results show that the Ge islands are less ordered for tilted Si(001) substrates. For substrates with a miscut of 25°, Ge dots nucleate on top of the ripples that form approximately perpendicular to the $[1-10]_{\text{Si}}$ direction, i.e., perpendicular to the step direction. Additionally, we observe the formation of Ge dashes, which align preferentially along the $[1-10]_{\text{Si}}$ direction. © 2005 American Institute of Physics. [DOI: 10.1063/1.1993751]

I. INTRODUCTION

As the dimensions of micro- and optoelectronic devices continue to shrink and the density of devices increases, different approaches for device structures and fabrication have been considered. An alternative approach to conventional lithography techniques is the spontaneous self-assembly of nanoscale structures which occurs during epitaxial growth of lattice mismatched materials such as Si/Ge and InGaAs/GaAs.¹

The formation of self-organized nanoscale structures in the Stranski-Krastanov growth mode is driven by the relaxation of strain, which is introduced by the lattice mismatch of substrate and epilayer.² For strain energies below a critical value, the growth progresses in a two-dimensional (2D) layer-by-layer mode and a wetting layer forms. If the critical strain energy is exceeded there is an onset of three-dimensional (3D) growth.

The strain energy of a SiGe layer grown pseudomorphically on Si depends on its thickness as well as on its composition. For a pure Ge the critical thickness of dot formation is reported to be between 3 and 6 monolayers (ML).^{3,4} Decreasing the Ge concentration reduces the strain energy that is due to the lattice mismatch between SiGe epilayer and the Si substrate. Hence, the thickness of the wetting layer increases with decreasing Ge concentration.^{2,3} After the onset of 3D growth, SiGe islands form. The shapes of these SiGe islands grown on Si(001) are prismatic or pyramidal with $\{105\}$ facets. The bases of these so-called “hut” clusters are rectangles with edges normal to the $\langle 100 \rangle$ direction.⁴ Prior studies have investigated the self-assembly of Ge dots on Si(001) substrates^{2,5} as well as on Si(001) substrates with surface normals rotated from the (001) axis towards the (111) axis by up to 4°. It was shown that these self-assembled Ge islands are weakly ordered when directly grown on vicinal Si(001) substrates. However, two-dimensional ordering of Ge islands is realized when Ge is deposited on a SiGe/Si multilayer.⁵

The driving force for the self-organization process is the interaction of strain fields induced by the buried islands. Ter-

soff *et al.*⁶ and Xie *et al.*⁷ proposed models for the vertical and lateral ordering of islands in the growth of superlattices. Tersoff *et al.*⁶ focused on the effects of strain on the nucleation of islands. The multilayers consist of successive layers of islands (i.e., buried islands) separated by Si spacer layers. A buried island leads to strain at the surface of the spacer layer, which reduces the lattice mismatch between this surface and the deposited material directly above the position of the buried island. Assuming that the formation of an island is most favorable in regions where the strain gives a minimum in the lattice mismatch, the favored nucleation position for an island is directly above a single-buried island. The regions of nucleation, i.e., the local minima in lattice mismatch, can be obtained by superposing the strain fields of all the buried islands. Tersoff *et al.*⁶ showed that for successive layers the island positions correlate in the vertical direction and the island size and spacing becomes progressively more uniform.

Qualitatively, Xie *et al.*⁷ obtained similar results for the vertical ordering by considering the effects of strain on diffusion, rather than focusing on the nucleation of the islands. The driving force for self-ordering in island systems is shown to be the island-induced strain fields which give rise to a preferred direction of adatom migration. The deposited adatoms are driven by the strain field to accumulate on top of the buried islands.⁷ This is also energetically favorable due to the reduced lattice mismatch of Ge and Si at positions above a buried island. The buried SiGe islands lead to strain at the surface of the Si spacer layer which reduces the mismatch between Si and the deposited Ge. The next layer islands nucleate at positions of minimum lattice mismatch, i.e., directly above a buried island.

Following the simplified model of island self-ordering in multilayer growth of Tersoff *et al.*,⁶ the island distribution at any stage depends mainly on the initial arrangement and the spacer layer thickness L . However, after many layers of growth the resultant island distribution is dependent only on the layer thickness and tends towards an interisland spacing of $\sim 3.5L$. For large initial island spacing, i.e., much greater than $3.5L$, the next layer islands form not only above the existing islands but also in the space between the islands.⁶

^{a)}Electronic mail: robert_nemanich@ncsu.edu

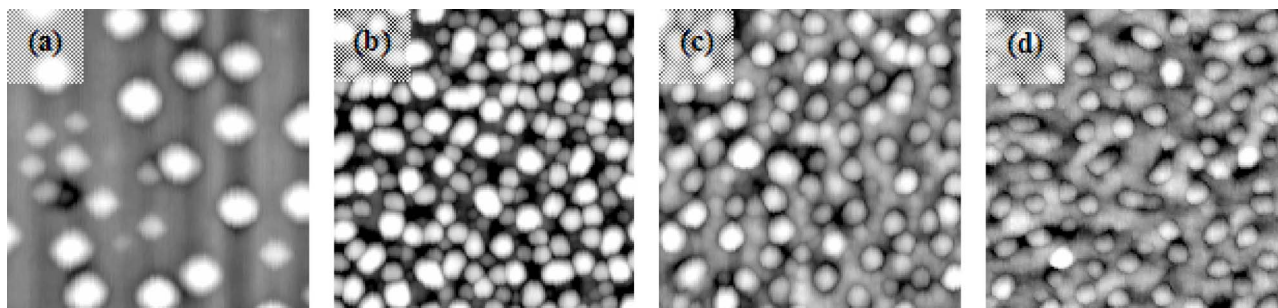


FIG. 1. $1 \times 1\text{-}\mu\text{m}^2$ AFM images of a single 25-Å-thick layer of $\text{Si}_{0.55}\text{Ge}_{0.45}$ grown at 550 °C on Si(001) substrates tilted by (a) 0°, (b) 2°, (c) 4°, and (d) 13°. The horizontal direction is approximately $[1-10]_{\text{Si}}$.

For islands that are closely spaced, two or more islands will be replaced by one single island in the next layer.⁶ Hence, after sufficiently many island layers, a uniform, characteristic island spacing determined by the spacer layer thickness will be achieved.

In this study we investigate the growth of the self-assembled Ge islands on Si(001) substrates with the surface normal inclined towards (111) by up to 25°. In particular, we confirm prior studies, which show a two-dimensional ordering of the Ge islands when a SiGe/Si multilayer is predeposited on Si(001) surfaces. For substrates with a miscut of 25° we observe the formation of elongated Ge islands that grow preferentially perpendicular to the $[1-10]_{\text{Si}}$ direction and Ge dots that nucleate on top of ripples that form parallel to the $[1-10]_{\text{Si}}$ direction.

II. EXPERIMENTAL PROCEDURE

The samples were grown by molecular-beam epitaxy in ultrahigh vacuum (UHV). Commercially available Si substrates were used with surface orientation off axis from (001) towards (111) by 0°, 2°, 4°, 10°, and 22°. After TEM examination of epitaxial SiGe layers grown on the 10° and 22° off-axis substrates, we concluded that the angles specified by the manufacturer were not accurate.⁸ TEM analysis indicated that the specified 10° surface was actually $\sim 13^\circ$ off-axis, and the specified 22° surface was actually $\sim 25^\circ$ off axis. Throughout this study, we will refer to these surfaces as 13° and 25° off axis in accordance with the TEM measurements. We note that the 13° surface is close to the (116) plane, and the 25° surface is close to the (113) plane.

The Si wafers were cleaned by UV-ozone exposure and a wet chemical clean using a 10:1 hydrofluoric acid solution diluted in de-ionized water. Following the *ex situ* clean, the wafers were introduced into the UHV transfer line through a load lock. The UHV transfer line connects multiple chambers for surface processing, film growth, and analysis. The films were prepared in a solid source molecular-beam epitaxy (MBE) system which consist of two electron-beam deposition sources (one with Si and one with Ge). The sources were separated by about 12 cm, and the source to the sample distance was about 25 cm resulting in near normal deposition.

After loading the wafers were transferred into the solid source MBE and submitted to a thermal treatment at 900 °C for 10 min. After cooling to 550 °C, and immediately prior to deposition of the SiGe/Si multilayers, a 20-nm Si buffer

layer was grown. Auger electron spectroscopy (AES) and low-energy electron diffraction (LEED) were used to confirm that the preparation technique was sufficient. The LEED showed a sharp (2×1) reconstruction of the Si(001) surface, and AES showed less than 1% carbon and 2% oxygen on the cleaned surface.

Ge islands were grown at 500 °C, either directly on the substrates or after predeposition of a SiGe/Si multilayer on Si(001) surfaces with a miscut of 0°, 2°, 4°, 13°, or 25° at 550 °C. If not otherwise specified, the multilayer consisted of 20 periods of 2.5-nm $\text{Si}_{0.55}\text{Ge}_{0.45}$ /10-nm Si bilayers. The growth parameters have been adopted from Ref. 3. The $\text{Si}_{0.55}\text{Ge}_{0.45}$ layers were formed by codeposition of Si and Ge in a UHV solid source MBE at a combined rate of 0.04 nm/s and at a surface temperature of 550 °C.

Raman scattering was conducted using the 514 and 458-nm lines of an Ar^+ -ion laser. The Si–Si Raman peak position from the layer was used to determine the strain in the SiGe layers. Ware⁹ demonstrated the use of Raman spectroscopy to determine the strain in a layer for off-axis substrates. Using the deformation potential calculations, Ware⁹ predicted the value of the Raman peaks for the Si–Si mode in strained films. The amount of relaxation in the layers can then be determine by taking a linear extrapolation between the bulk relaxed Raman peak position and the calculated pseudomorphically strained values. Raman spectra from several samples indicated the Si–Si mode at 505 cm^{-1} . The value for bulk-relaxed $\text{Si}_{0.55}\text{Ge}_{0.45}$ is 490 cm^{-1} . Employing this technique we determined the SiGe layers to be $95\% \pm 3\%$ strained.

Atomic force microscopy (AFM) was employed to determine the surface morphology. All measurements were performed in ambient using a Thermo Microscope CP system and silicon nitride tips.

III. RESULTS

A. Growth on Si(001) with 0°–13° miscut

Figure 1 shows AFM images of a 2.5-nm-thick $\text{Si}_{0.55}\text{Ge}_{0.45}$ layer grown on Si(001) substrates with surface normals rotated towards (111) by 0°, 2°, 4°, and 13°, respectively. We observe the formation of SiGe islands in all cases. However, the AFM images reveal a change in island density, island structure, and surface morphology for the different stepped surfaces.

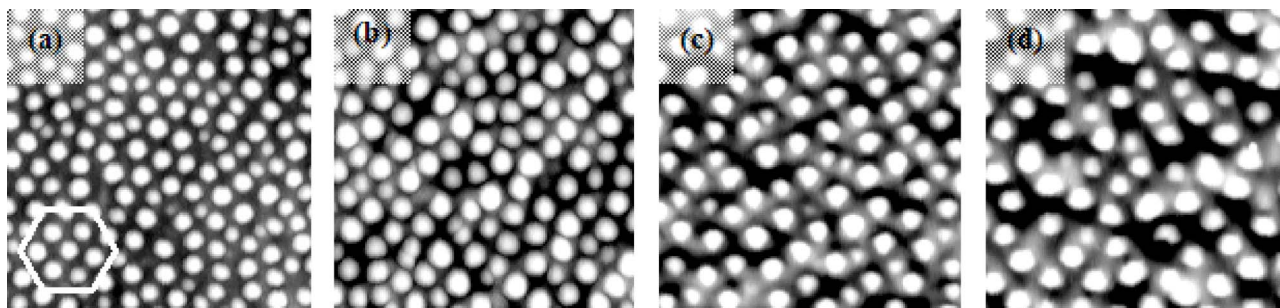


FIG. 2. $2 \times 2\text{-}\mu\text{m}^2$ AFM images of Ge islands ($8.5\text{-}\text{\AA}$ Ge coverage) on a sample with a SiGe/Si multilayer and Si(001) substrates tilted by (a) 0° , (b) 2° , (c) 4° , and (d) 13° . The gray scale range is 100 \AA in (a) and (c), 130 \AA in (b), and 120 \AA in (d) with light meaning high. The framed area in (a) indicates the hexagonal ordering of Ge islands. The horizontal direction is approximately $[1-10]_{\text{Si}}$.

For nominally on-axis Si(001) surfaces the SiGe dots are relatively large, while for 2° off-axis substrates they are smaller and more dense. In the cases of 4° and 13° off-axis substrates we observe the formation of even smaller dots, with a decreased areal density, and the dots are formed in valleys of the underlying layer. At least between the dots, the SiGe wetting layer apparently grows thicker for the 4° and 13° miscut substrates. These undulations indicate another instability of the strained wetting layer.

The structure of the SiGe dots on the nominally flat Si(001) surface appears pyramidal to within the resolution of the AFM used in this study. Higher-resolution AFM images of individual islands indicate that the bases of the pyramidal SiGe islands are squares with edges normal to the $\langle 100 \rangle$ directions. A line scan along the $\langle 100 \rangle$ directions reveals that the sides of the islands are tilted with respect to the (001) plane by $11^\circ \pm 2^\circ$. Hence, these islands are bound by $\{105\}$ facets and resemble the so-called hut clusters referred to previously.⁴

The structure of the SiGe islands that form on vicinal Si(001) substrates with surface normals rotated from (001) towards (111) by 2° , 4° , and 13° , respectively, differs from the hut structure typically found for SiGe islands on nominally flat Si(001). Higher-resolution images of individual islands did not display island edges oriented along the $\langle 100 \rangle$ direction. Moreover, the slope of the island sides appears to be steeper than the slope of the hut clusters suggesting a different facet structure. Hence, the morphology of the islands on the first SiGe layer varies for the different stepped surfaces and will influence the growth processes of the additional layers.

To explore the self-ordering process on the off-axis substrates, Ge islands were grown after predeposition of a SiGe/Si multilayer. Figure 2 shows the AFM images of Ge islands grown on a $\text{Si}_{0.55}\text{Ge}_{0.45}/\text{Si}$ 20 period superlattice for Si(001) substrates with surface normals rotated towards (111) by 0° , 2° , 4° and 13° , respectively. For nominally on-axis Si(001) surfaces, visual inspection of the images indicates a lateral self-ordering of the Ge islands when grown on a SiGe/Si superlattice, which has been reported previously.^{2,5} The Ge islands trend towards a 2D hexagonal pattern, as indicated by the white frame in Fig. 2(a). The AFM image also reveals a rather uniform island size distribution. Comparing this with the results of a single $\text{Si}_{0.55}\text{Ge}_{0.45}$ layer, shown in Fig. 1(a), we find the island size and the island

spacing to be much more uniform for the multilayer sample. The island size distribution appears to be bimodal for the first SiGe layer. However, the size distribution of the Ge islands that are grown on top of the SiGe/Si multilayer is monomodal and narrower. This indicates improved ordering of Ge islands grown on stacks of islands separated by a Si spacer layer, as predicted and shown by Tersoff *et al.*⁶ and Teichert *et al.*¹⁰

Figures 2(b)–2(d) show AFM images of the samples with a SiGe/Si multilayer and a Ge coverage of 8.5 \AA grown on 2° , 4° , and 13° tilted Si(001) substrates, respectively. For these tilted substrates the degree of ordering of the islands also increases when grown on multilayers, similar to the on-axis Si(001) samples. The islands have a similar lateral dimension in all cases, but the density appears to decrease somewhat with increased tilt, and enhanced undulations become apparent. Moreover, the Ge islands are found to be less ordered and their size to be less homogeneous for higher miscut angles. For 13° tilted Si(001) substrates, shown in Fig. 2(d), the ordering of Ge islands is weak.

The morphology differences of the topmost Ge layer grown on the superlattice samples with different tilt angles indicate that the ordering process is dependent on the initial arrangement of the islands, i.e., the morphology of the first SiGe layer, and hence, on the surface orientation of the substrate.

B. Growth on Si(001) with 25° miscut

Using Si(001) substrates with surface normals inclined towards (111) by 25° , we find a transition from a dot structure to a ripple structure for the first 2.5-nm SiGe layer. Figure 3(a) shows an AFM image of one SiGe layer deposited on a Si(001) substrate with 25° miscut. The ripples align approximately perpendicular to the $[1-10]_{\text{Si}}$ direction, i.e., perpendicular to the step direction.

To explore the growth of Ge islands on a superlattice for these 25° miscut Si(001) substrates, we deposited three periods of $\text{Si}_{0.55}\text{Ge}_{0.45}/\text{Si}$ at 550°C and a final layer (8.5 \AA) of Ge at 500°C . The AFM image of the topmost layer of this sample [Fig. 3(b)] also shows a ripple structure and Ge dots that form preferentially on top of these ripples.

A similar experiment was performed with a 20-period $\text{Si}_{0.55}\text{Ge}_{0.45}/\text{Si}$ multilayer. The AFM images of this sample are shown in Figs. 4(b)–4(d). We find ripples perpendicular

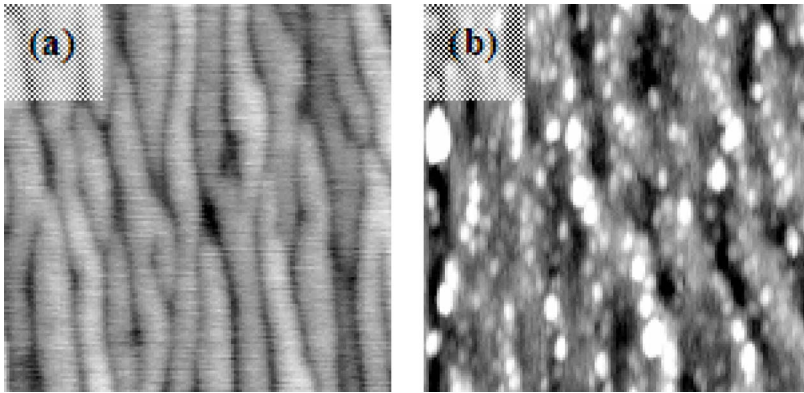


FIG. 3. $1 \times 1\text{-}\mu\text{m}^2$ AFM images of (a) a single 25-Å $\text{Si}_{0.55}\text{Ge}_{0.45}$ layer and (b) 8.5-Å Ge deposited onto a superlattice of three periods of $\text{Si}_{0.55}\text{Ge}_{0.45}/\text{Si}$. All samples are grown on Si(001) substrates tilted by 25° towards (111). The horizontal direction is approximately $[1-10]_{\text{Si}}$.

to the $[1-10]_{\text{Si}}$ direction. However, the ripple structure of the topmost layer is strongly correlated to the undulations of the last Si spacer layer shown in Fig. 4(a). This shows that for these larger scale structures the Si does not planarize over each layer. In addition, we find the formation of Ge dots and Ge dashes, i.e., elongated islands. The Ge dots nucleate preferentially on top of the ripples and form stripes perpendicular to the $[1-10]_{\text{Si}}$ direction. The average density of these dots decreases around most of the relatively large Ge dashes.

The Ge dashes align preferentially along the $[1-10]_{\text{Si}}$ direction, i.e., perpendicular to the direction of the ripples. For a Ge coverage of 8.5 Å the dashes were ~ 270 nm wide and up to $1\ \mu\text{m}$ long. A 3D AFM image of one of these dashes is shown in Fig. 5. As is evident, the facet structure is complex, and could not be reliably determined from our images. We find that one end of the dash is often relatively enhanced in comparison to the elongated part. It is suggestive that the enhanced height end could represent a dome structure which was elongated during the coarsening and growth processes. This type of height difference across the Ge dash was found for most of the elongated islands. From our limited observations we have not determined if there is a preferential orientation for the enhanced height end.

To investigate the influence of the growth temperature we prepared two 20 period $\text{Si}_{0.55}\text{Ge}_{0.45}/\text{Si}$ superlattice samples with a topmost Ge layer of 6 and 10 Å, respectively, and increased the Ge deposition temperature to 525°C . Figure 6 shows the AFM images of these samples. We observe the formation of Ge dots and dashes. However, the density of the Ge dashes depends on the deposition temperature as well as on the Ge coverage. An increase of the deposition tem-

perature from 500 to 525°C results in a reduction of the density of dashes. We also find that the number of dashes per unit area decreases if the Ge coverage increases from 6 to 10 Å. For both samples Ge dots and dashes form on a ripple structure as observed for the samples grown at 500°C .

However, the ripples are less regular and broader in the case of higher deposition temperature. The size of the Ge dots depends on the Ge coverage. Comparing the two samples of 6 and 10 Å Ge, we find that the size of the dots increases by more than a factor of 2.

IV. DISCUSSION

A. Si(001) with 0° to 13° miscut

For Si(001) substrates with surface normals rotated from (001) toward (111) by 0° , 2° , 4° , and 13° we find the self-ordering of Ge dots when grown on a SiGe/Si multilayer. However, the degree of ordering of Ge dots on a 20 period SiGe/Si superlattice decreases with increasing miscut angle. We anticipate that this is due to the degree of ordering in the initial SiGe layer, which decreases with increasing miscut angle. For nominally flat Si(001) substrates SiGe dots form on top of a thin flat wetting layer. When rotating the substrate surface from (001) towards (111) by 13° , the wetting layer is found to be thicker and undulated. Here, the Ge dots appear to form preferentially in valleys of the wetting layer.

The miscut of the substrate plays a crucial role in the ordering process: We find that the degree of ordering decreases with increasing miscut angle. Based on the results of Brunner *et al.*,¹¹ we anticipate that material deposited onto the stepped substrate collects at the surface steps, which

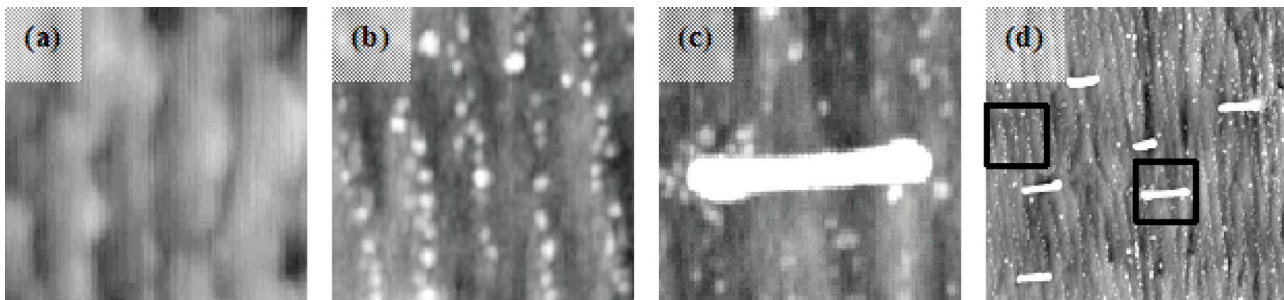


FIG. 4. AFM images of (a) the last 25-Å $\text{Si}_{0.55}\text{Ge}_{0.45}$ layer of the 20 period SiGe/Si superlattices and (b)–(d) 8.5-Å Ge deposited on the superlattice with the Si(001) substrates tilted by 25° towards (111). Size: (a)–(c) $1 \times 1\ \mu\text{m}$ and $5 \times 5\ \mu\text{m}$. The framed areas are shown in (b) and (c), respectively. The horizontal direction is approximately $[1-10]_{\text{Si}}$.

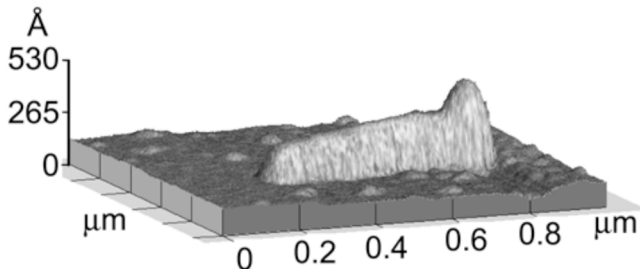


FIG. 5. $1 \times 1\text{-}\mu\text{m}^2$ AFM images of an elongated Ge island grown at $525\text{ }^\circ\text{C}$ on a 20 period $\text{Si}_{0.55}\text{Ge}_{0.45}$ superlattice with the Si(001) substrates tilted by 25° towards (111). The island is elongated in the $[1-10]_{\text{Si}}$ direction.

would result in strain relaxation around the steps. Hence, the early stage of stress relief of the strained material is due to the Ge at the surface steps.¹² The formation of Ge islands represents a later stage of strain relief. The strain relaxation due to the Ge at the steps results in a reduction of the stress pattern in the Si epitaxial layer. Hence, the Ge islands that assemble on top are less ordered when grown on stepped substrates.

We note that we did not observe the lateral ordering of the Ge islands on the 2° miscut surface as has been observed by Zhu *et al.*¹³ In that report the superlattice structures were grown on a surface miscut by 1.5° where the substrate surface had been prepared to exhibit a single domain surface reconstruction with biatomic steps. We expect that the lateral ordering observed in that study was related to the highly ordered step and terrace structure.

It has been shown that the degree of ordering increases with the number of layers in the superlattice.⁶ Tersoff *et al.*⁶ found that after the deposition of a sufficient number of layers, the ordering becomes less sensitive to the initial arrangement. Hence, we anticipate that the ordering of Ge dots grown on miscut Si(001) samples can be further improved if the number of successive SiGe/Si layers is increased.

B. Si(001) with 25° miscut

For Si(001) substrates with surface normals rotated from (001) toward (111) by 25° we find the formation of a ripple structure in the initial SiGe layer. The ripples align perpendicular to the $[1-10]_{\text{Si}}$ direction, i.e., perpendicular to the step direction. We anticipate that the morphological change from island to ripple structure in the first SiGe layer is due to the change of the structure of the initial Si surface. Si surfaces from (001) to (114), (i.e., 0° – 19.5°), reconstruct into (2

$\times 1$) (001) terraces, which are separated by single or double steps. For surfaces with higher miscut angle this morphology breaks down and the surface reconstructs into mesoscale facets composed of (113) and (114) surfaces.¹² Based on the prior TEM measurements,⁸ it would appear that the surface is composed largely of (113) facets. For the growth of SiGe layers on these highly vicinal substrates, prior studies from at least two groups have displayed the formation of surface undulations that are perpendicular to the step direction.^{9,14,15} In the step flow growth mode, the formation of the ripples is related to strain relaxation. For a surface with predominantly $[1-10]$ steps, kinetic effects can lead to coherent waviness in the step edges which would result in a ripple pattern nearly perpendicular to the step direction.

After the deposition of three periods of $\text{Si}_{0.55}\text{Ge}_{0.45}/\text{Si}$ the final Ge layer also shows a ripple structure and Ge dots that form preferentially on top of these ripples. We can conclude that the modulated strain field induced by the underlying structures propagates through the Si spacer layer. Hence, the Si spacer layer acts to create a strain distribution that is favorable for the formation of regularly spaced ripples. The strain field drives the directed diffusion of the deposited Ge adatoms to positions above the buried ripples, and these peaked regions are also more favored for nucleation of the Ge island structures.

For the 25° off-axis substrates we find the formation of Ge dashes and dots on top of the 20 period multilayers. The dots appear to be similar to those observed on the three period multilayers. The decrease of the average density of these dots around most of the Ge dashes indicates that coarsening processes play an important role in the formation of the Ge dashes.

The height profile of the dashes seems to give insight into their formation. The height profile shows a relatively tall islandlike end for most of the Ge dashes, and we anticipate that the large Ge islands form first and then elongate into the dash structures. This further growth and elongation is apparently governed by Ostwald ripening, where these islands elongate into the $[1-10]_{\text{Si}}$ direction and other nearby islands disappear or are consumed. It is not completely understood why elongated islands form on this surface. In the case of commensurate growth the lattice mismatch strain of an island increases with the size of the island. It is possible that strain relaxation drives the elongation of large islands as proposed by Tersoff and Tromp.¹⁶ In the case of strained island growth the lattice mismatch strain of an island increases with

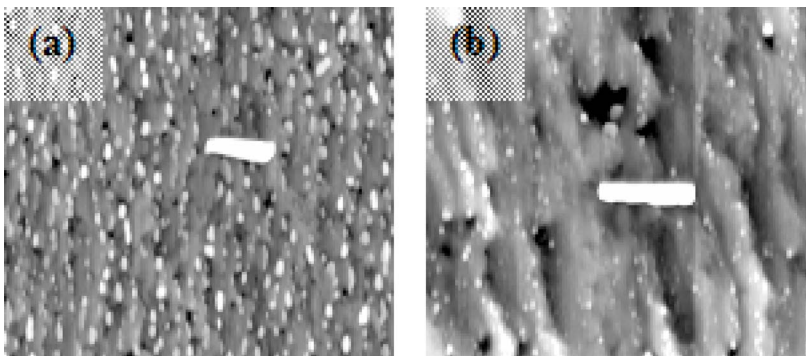


FIG. 6. $4 \times 4\text{-}\mu\text{m}^2$ AFM images of 10-Å Ge deposited at $525\text{ }^\circ\text{C}$ on a 20 period $\text{Si}_{0.55}\text{Ge}_{0.45}$ superlattices with the Si(001) substrates tilted by 25° towards (111). The horizontal direction is approximately $[1-10]_{\text{Si}}$.

the size of the island, and at one point it becomes more favorable to increase the surface energy through elongation of the island. We might also suggest that the large island is dislocated along the $[1-10]$ direction, and therefore elongation of the island in this direction would lower the energy. Specific facet structures may also play a role, but the complicated facet structure of the initial dome may not favor a single direction. It is evident that further research is necessary to understand the energetics and kinetics of these structures.

V. CONCLUSIONS

We studied the ordering of self-assembled Ge islands on SiGe/Si superlattices grown on miscut Si(001) substrates. For nominally flat Si(001) surfaces we find a 2D hexagonal ordering consistent with prior studies. The ordering process is strongly influenced by the orientation of the substrate. The self-assembled Ge dots on miscut Si(001) are less ordered and their size distribution is less homogeneous. Deposition of Ge on top of superlattices for substrates with a miscut up to 13° results in an increase in the island ordering, but the final structures are still less ordered than those grown on (001) substrates. In contrast, for deposition on substrates with a miscut of 25° , Ge dots are observed to form on top of the ripples, which are oriented perpendicular to the step direction. In addition, elongated Ge islands are found which are aligned along the $[1-10]_{\text{Si}}$ direction. The growth of the elongated islands is apparently mitigated by ripening pro-

cesses. It is anticipated that strain relaxation contributes to the formation of the elongated islands, but the detailed mechanism has not been determined.

ACKNOWLEDGMENT

This research is supported by the National Science Foundation under Grant No. DMR-0102652.

- ¹H. Omi and T. Ogino, Appl. Phys. Lett. **71**, 2163 (1997).
- ²P. Schittenhelm, G. Abstreiter, A. Darhuber, G. Bauer, P. Werner, and A. Kosogov, Thin Solid Films **294**, 291 (1997).
- ³G. Abstreiter, P. Schittenhelm, C. Engel, E. Silveira, A. Zrenner, D. Meertensand, and W. Jäger, Semicond. Sci. Technol. **11**, 1521 (1996).
- ⁴Y.-W. Mo, D. E. Savage, B. S. Swartzentruber, and M. G. Lagally, Phys. Rev. Lett. **65**, 1020 (1990).
- ⁵J.-H. Zhu, K. Brunner, G. Abstreiter, O. Kienzle, and F. Ernst, Thin Solid Films **336**, 252 (1998).
- ⁶J. Tersoff, C. Teichert, and M. G. Lagally, Phys. Rev. Lett. **76**, 1675 (1996).
- ⁷Q. Xie, A. Madhukar, P. Chen, and N. P. Kobayashi, Phys. Rev. Lett. **75**, 2542 (1995).
- ⁸M. E. Ware, R. J. Nemanich, J. L. Gray, and R. Hull, J. Appl. Phys. **95**, 115 (2003).
- ⁹M. E. Ware, Ph.D. Dissertation, North Carolina State University, 2002.
- ¹⁰C. Teichert, M. G. Lagally, L. J. Peticolas, J. C. Bean, and J. Tersoff, Phys. Rev. B **53**, 16334 (1996).
- ¹¹K. Brunner, J. Zhu, C. Miesner, G. Abstreiter, O. Kienzle, and F. Ernst, Physica E (Amsterdam) **7**, 881 (2000).
- ¹²A. A. Baski, S. C. Erwin, and L. J. Whiteman, Surf. Sci. **392**, 69 (1997).
- ¹³J.-h. Zhu, K. Brunner, and G. Abstreiter, Appl. Phys. Lett. **73**, 620 (1998).
- ¹⁴A. Ronda, M. Abdallah, J. M. Gay, J. Stettner, and I. Berbezier, Appl. Surf. Sci. **162–163**, 576 (2000).
- ¹⁵I. Berbezier, A. Ronda, and A. Portavoce, J. Phys.: Condens. Matter **14**, 8283 (2002).
- ¹⁶J. Tersoff and R. M. Tromp, Phys. Rev. Lett. **70**, 2782 (1993).